*Materials Transactions*, Vol. 48, No. 9 (2007) pp. 2285 to 2288
Special Issue on Solidification Science and Processing for Advanced Materials


# Faceted Crystal Growth of Silicon from Undercooled Melt of Si-20 mass%Ni Alloy

Tsukasa Takazawa*, Minoru Ikeda and Toshio Suzuki

*Department of Materials Engineering, The University of Tokyo, Tokyo 113-8656, Japan*

Two-dimensional faceted crystal growth of silicon from undercooled melt of Si-20 mass%Ni alloy was experimentally investigated, in which a droplet sample from 10 to 100 mg was undercooled on a single-crystal sapphire and growing crystals were observed in situ. Observed crystals were classified according to the shapes of square, wedge and irregular shapes. The growth velocity was measured for different undercooling conditions. The growth velocity of square shaped crystals was about half times smaller than that of wedge shaped crystals. The growth of square shaped crystals is regarded to be two-dimensional and it is compared with the results of two-dimensional phase-field simulations. Growth velocity in both is in good agreement and the linear kinetic coefficient is estimated to be 0.002 m/sK.
[doi:10.2320/matertrans.MB200709]

(Received February 27, 2007; Accepted May 14, 2007; Published August 25, 2007)

***Keywords:*** *faceted crystal growth, silicon, undercooling, phase-field models*

## 1. Introduction

Half a century ago, faceted dendrite growth of germanium was first reported by Billig[1] and its crystallographic aspects were investigated aiming the production of semiconductor ribbons.[2,3] Because of the rapid progress of silicon wafer production technology the interest in faceted dendrite growth was subsided for many years until Devaud and Turnbull[4] found a twin-free dendrite in the late 1980s. Thereafter, intensive investigations on faceted free dendrite growth of germanium, silicon, and their alloys were carried out using the glass flux technique[4–8] or electromagnetic levitation technique[9–16] and the crystallographic morphology of solidified crystals was examined. The growth velocity of faceted dendrites was also measured for germanium, silicon, and their alloys[8–16] and the measured growth velocity was analyzed using an analytical dendrite model termed such as the BCT model[17] or the LKT model.[18]

In the meantime phase-field approaches to faceted crystal growth were proposed so as to include highly anisotropic interface energy[19,20] or interface kinetics.[21] In usual phase-field approaches, the solidification interface energy, $\sigma(\theta)$, is simply assumed to have fourfold symmetric anisotropy given as,

$$\sigma(\theta) = \sigma_0(1 + \nu \cos 4\theta)$$

where $\nu$ is the intensity of anisotropy and $\theta$ is the angle between the direction normal to the interface and a fixed axis. The equilibrium condition at the interface is given by the Gibbs-Thomson equation. When $\nu < 1/15$, a smooth and convex non-faceted crystal becomes stable. Conversely when $\nu > 1/15$, the interface within the missing orientation becomes thermodynamically unstable, the faceted crystal appears to be composed of only interfaces with stable orientations. Eggleston *et al.*[19] proposed modification of the governing equation. The interface energy within the missing orientations was changed using that of the interface at the end of the stable orientations and the model successfully reproduces the equilibrium shape and the transient growth toward the equilibrium state of a faceted interface. Debierre *et al.*[20] proposed a different type of anisotropic interface energy in their phase-field approach. They performed phase-field simulations of faceted dendrite growth with vanishing interface kinetics. Kasajima and coworkers[22,23] carried out phase-field simulations of free faceted dendrite growth of silicon using the interface energy model by Eggleston *et al.* and thin interface limit parameters. Their results were similar to those by Debierre *et al.* and it indicated that both approaches could be applicable to real systems with faceted crystals such as silicon.

However, there are difficulties in the phase-field simulation of silicon dendrite growth. The capillarity length of silicon is so small that the mesh size should be less than 1 nm so as to obtain correct values of dendrite growth velocity. Therefore, three-dimensional simulation of silicon dendrite growth is impracticable and the agreement between two-dimensional phase-field simulations and experimental data is still unsatisfactory. These difficulties would be reduced if data on the two-dimensional faceted crystal growth of silicon alloys could be provided. Two-dimensional experiments of dendrite growth are generally difficult to perform but the present authors found silicon crystals grow along the free surface of the molten silicon or silicon alloy at small undercooling. Therefore, it becomes possible to compare the results of two-dimensional faceted crystal growth experiments with phase-field simulations. In the present work faceted silicon crystals grown from the undercooled melt of silicon-nickel alloy are observed in situ and dendrite growth velocity is measured for different undercooling conditions. Finally, the growth velocity is compared with two-dimensional phase-field simulations.

## 2. Experimental

The Si-20 masst%Ni alloy was prepared from semiconductor grade silicon and 99.99% nickel. Figure 1 shows the experimental setup used in the experiments. A specimen with

*Graduate Student, The University of Tokyo, Present address: The Furukawa Electric Co. Ltd.

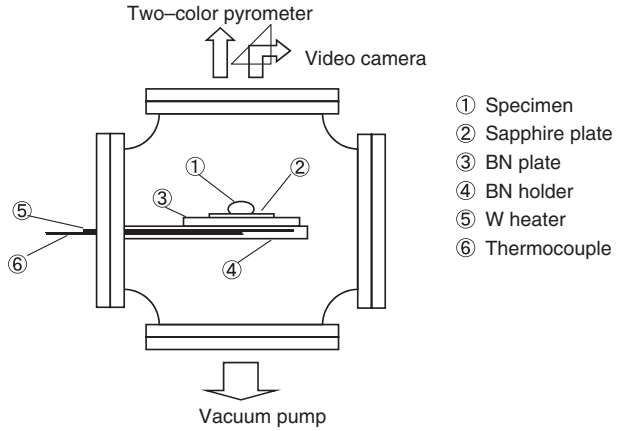


Fig. 1 Experimental set-up.

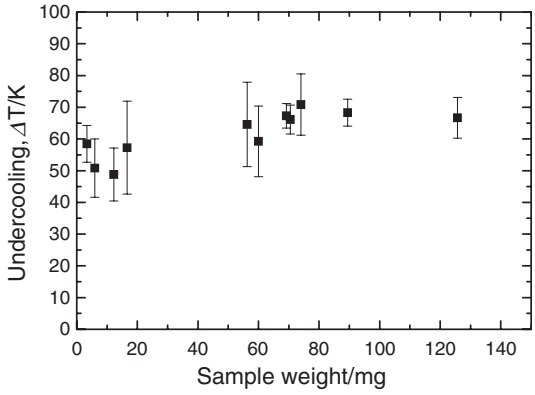


Fig. 2 Average undercooling vs. sample weight.

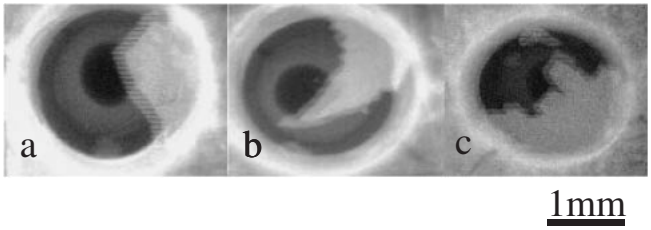


Fig. 3 Different types of observed crystals. (a) Type A, (b) Type B and (c) Type C.

a mass from ten to hundred mg was placed on a single-crystal sapphire plate with a $(10\bar{1}0)$ surface. It was melted under a Ar+5%$H_2$ atmosphere of $10^{-1}$ Pa using a resistance furnace with a tungsten plate heater. The specimen was heated up to the temperature of 30 K above the liquidus temperature and then continuously cooled with a constant cooling rate of about 5 K per minute until nucleation spontaneously started. During the heating process the solute content of the alloy was examined by measuring the liquidus temperature. The degree of undercooling in each experimental run was determined as the difference between the liquidus temperature and the nucleation temperature measured by a two-color pyrometer. The error of measured undercooling was expected to be within 5 K at most, including the variation of nickel content.

As the emissivity of silicon is sufficiently different for the solid and liquid phases, growing crystals can be optically identified. For the observation of crystal growth, a digital video camera attached with a 300 mm telescopic lens was used. The recorded images were processed to increase their contrast and the growth velocity was measured for each experimental run. Note that an image recorded by the television frame rate consisted of two frames scanned every 1/60 seconds and the growth distance in 1/60 second was easily read out from an image. After the experiments, the crystallographic orientations analysis using a SEM-EBSP was carried out for typical samples. Two-dimensional phase-field simulations for the crystal growth of silicon were performed so as to evaluate the value of interface kinetic coefficient. The details of governing equations, phase-field parameters and physical properties of the alloy can be found elsewhere.[24)]

## 3. Results and Discussions

Figure 2 shows the relationship between undercooling and sample weight. The average undercooling slightly increases with increase of sample weight. Though it falls within the range of undercooling from 50 to 70 K, the results of measured undercooling for different sample weights show a wide distribution. It is presumably due to the fact that surface roughening during heating produces macro steps on the sapphire surface and they act as nucleation sites with different potentials.

The morphology of growing crystals is classified into three types according to their shapes as shown in Fig. 3. The first type is the crystal with a square shape (Type A). It is a typical facetted crystal with plane interfaces whose corner angle is about 110 degree. The crystallographic orientations analysis using a SEM-EBSP shows that it has the ⟨111⟩ interface planes and grows along the (110) face. Though the equilibrium solid fraction of the alloy in the range of obtained undercooling is small, the crystal of Type A grows covering the free surface of the sample. Therefore it presumably is a thin plate-like crystal and it grows along the free surface of the sample. The second one (Type B) is a wedge shaped crystal. It grows in the ⟨212⟩ direction, and its tip angle of the wedge is about 60 degrees. It is presumably a ⟨211⟩ twin dendrite reported by Nagashio and Kuribayashi,[25)] though the growth plane seems to be slightly inclined to the free surface. The third one (Type C) has an irregular shape and looks as the mixture of plural crystals.

Figure 4 shows the histogram of the types of grown crystals at different undercooling. Though the nucleation on a sapphire plate randomly occurs, the crystal with the preferred growth plane is presumably selected during their growth along the free surface. Therefore most crystals grow having the growth plane of (110) or (111), and about 70% of observed crystals is such a crystal classified in Type A or B. However a ⟨211⟩ dendrite of Type B is a narrow tip width and does not necessarily grow parallel to the free surface.[26)] The Type C crystals are apparently plural crystals and have no clear crystallographic characteristic.

Figure 5 shows the relationship between growth velocity and undercooling. In the figure, open circles, plus and cross symbols show the growth velocities of Type A, B and C crystals respectively. The experimental data are widely

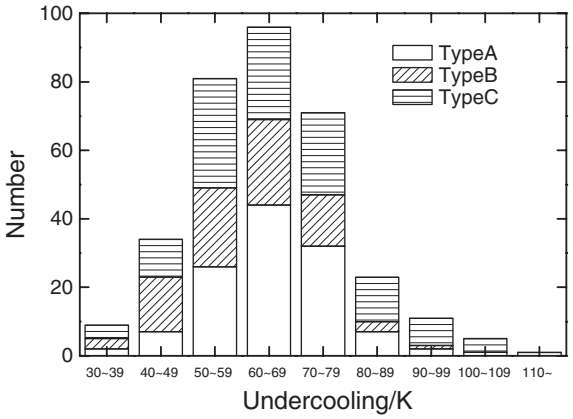


Fig. 4 Histogram of crystal types for different degrees of undercooling.

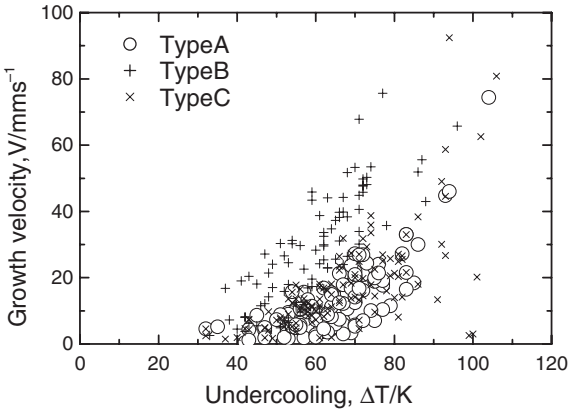


Fig. 5 Growth velocity vs. undercooling. Open circles, plus and cross symbols show the growth velocities of Type A, B and C crystals, respectively.

scattered, and the correct growth velocity for each type of crystals is estimated from the upper envelope of the data.[27] The growth velocity of Type B crystals is about two times larger than that of Type A crystals. As described above, Type A crystals grow along the free surface with a thin plate-like shape and thus their growth is regarded to be the two-dimensional growth whose symmetry plane is the free surface of the sample. On the contrary, the growth of Type B crystals is not necessarily two-dimensional, because its growth plane is inclined to the free surface and it grows slightly beneath the surface. Therefore the growth velocity of Type A crystals can be compared with two-dimensional phase-field simulations. Namely, the shape of a Type A crystal from the top view is a square-like shape and the characteristic length of its edge is much larger than the tip size of the growing plate-like crystal at the longitudinal cross section perpendicular to the free surface. Therefore the shape effect of the edge for the crystal shape from the top view could be negligible and the growth of a Type A crystal can be approximated to be the two-dimensional growth. In the two-dimensional phase-field simulations, the growth conditions for a Type A crystal could be satisfied by taking the preferred growth direction of the crystal to be the x-axis and by applying the symmetric boundary conditions along the x-axis.

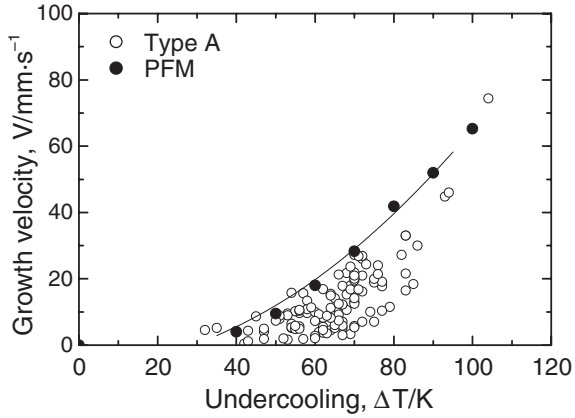


Fig. 6 Growth velocity of Type A crystals vs. undercooling. Open circles are the experimental data, and colosed circles and a solid line show the results of phase-filed simulations with $\mu = 0.002$ m/sK.

Phase-field simulations for the faceted crystal growth of silicon from the undercooled melt of Si-20 mass%Ni alloy has been carried out under the corresponding experimental conditions. In the simulations it is assumed that the system is isothermal and the growth of a crystal is dominated by solute diffusion. The results calculated with the linear kinetic coefficient of 0.002 m/sK are shown as closed circles and solid line in Fig. 6. The calculated growth velocity follows a similar power relationship to undercooling to experiments. In the model the fourfold symmetry of interface energy is assumed but both are in good agreement when the upper envelope of the experimental data is concerned. The values of linear kinetic coefficient for ⟨100⟩ and ⟨111⟩ faces of silicon have been obtained by numerical simulations[28,29] or experiments,[30–32] and most of the data for a (100) face of silicon are in the range from 0.2 to 0.05 m/sK. The value of linear kinetic coefficient for a Si-6 mass%Ni alloy is reported to be 0.01 m/sK[33] and it is supposed to becomes small with increase of solute content because the driving force for solute partition at interface would be necessary. Therefore the value of linear kinetic coefficient used in the simulation is acceptable and the agreement between simulations and experiment show that the conditions in the simulations have been appropriately assumed.

## 4. Conclusions

A detailed investigation on a faceted crystal growth of silicon from the undercooled melt of Si-20 mass%Ni alloy was conducted. In the experiments a small droplet of molten silicon-nickel alloy was undercooled from 30 to 110 K. The morphology of growing crystals was in-situ observed and it was classified into three types of square shaped, wedge shaped and irregular crystals. Crystallographic analysis and microscopic observations reveals that square shaped crystals are plate-like ones and grow along the free surface of the sample. Growth velocity for each type of crystals was measured at different undercooling. The growth velocity of square type crystals is half times smaller than that of wedge type crystals, though the measured growth velocity data are widely scattered. The upper envelope of the growth velocity

data for square type crystals follows a power relationship to undercooling with its exponent of about 2. It is compared with two-dimensional phase-filed simulations the value of kinetic coefficient is estimated to be 0.002 m/sK.

## Acknowledgement

This work was supported by the Grant-in-Aid for Scientific Research (A) (Grant No. 17206072) from the Ministry of Education, Culture, Sports, Science and Technology, Japan.

## REFERENCES

1) E. Billig: Proc. Roy. Soc. A **229** (1955) 346.
2) D. R. Hamilton and R. G. Seidensticker: J. Appl. Phys. **31** (1960) 1165.
3) R. S. Wagner: Acta Metall. **8** (1960) 57.
4) G. Devaud and D. Turnbull: Acta Metall. **35** (1987) 765.
5) C. F. Lau and H. W. Kui: Acta Metall. Mater. **39** (1991) 323.
6) C. F. Lau and H. W. Kui: Acta Metall. Mater. **41** (1993) 1999.
7) C. F. Lau and H. W. Kui: Acta Metall. Mater. **42** (1994) 3811.
8) S. E. Battersby, R. F. Cochrane and A. M. Mullis: J. Mater. Sci. **34** (1999) 2049.
9) D. Li, T. Volkmann, K. Eckler and D. M. Herlach: J. Crystal Growth **152** (1995) 101.
10) D. Li and D. M. Herlach: Phys Rev. Lett. **77** (1996) 1801.
11) D. Li, K. Eckler and D. M. Herlach: Acta Mater. **44** (1996) 2437.
12) R. P. Liu, T. Volkmann and D. M. Herlach: Acta Mater. **49** (2001) 439.
13) T. Aoyama, Y. Takamura and K. Kuribayashi: Metall. Mater. Trans. A **30** (1999) 1333.
14) Aoyama and K. Kuribayashi: Acta Mater. **48** (2000) 3739.
15) T. Aoyama and K. Kuribayashi: Mater. Sci. Eng. A **304** (2001) 231.
16) T. Aoyama and K. Kuribayashi: Acta Mater. **51** (2003) 2297.
17) W. J. Boettinger, S. R. Coriell and R. Trivedi: *Rapid Solidification Processing: Princeples and Technologies IV*, ed by R. Mehrabian, P. A. Parrish, (Claitor's Baton Rouge, 1988) 13.
18) J. Lipton, W. Kurz and R. Trivedi: Acta Metall. **35** (1987) 957.
19) J. J. Eggleston, G. B. McFadden and P. W. Voorhees: Physica D **150** (2001) 91.
20) J.-M. Debierre, A. Karma, F. Celestini and R. Guerin: Phys. Rev. E **68** (2003) 041604.
21) T. Uehara and R. F. Sekerka: J. Crystal Growth **254** (2003) 251.
22) H. Kasajima, E. Nagano, T. Suzuki, S. G. Kim and W. T. Kim: Sci. Tech. Adv. Mater. **4** (2003) 553.
23) H. Kasajima, T. Suzuki, S. G. Kim and W. T. Kim: J. Mater. Res. Soc. Japan **29** (2004) 3779.
24) T. Suzuki, S. G. Kim and W. T. Kim: Mater. Sci. Eng. A, **449–551** (2007) 99.
25) K. Nagashio and K. Kuribayashi: Acta Mater. **53** (2005) 3021.
26) K. Nagashio: private communication.
27) T. Suzuki, S. Toyoda, T. Umeda and Y. Kimura: J. Crystal Growth **38** (1977) 123.
28) M. H. Grabow, G. H. Gilmer and A. F. Baker: MRS Symp. Proc. **141** (1989) 349.
29) K. M. Beatty and K. A. Jackson: J. Crystal Growth **211** (2000) 13–17.
30) M. Iwamatsu and K. Horii: Physics Lett. A **214** (1996) 71–75.
31) G. J. Galvin, J. W. Mayer and P. W. Peercy: Appl. Phys. Lett. **46** (1985) 644
32) G. D. Ivlev and E. I. Gatskevich: Appl. Surface Sci. **143** (1999) 265–271.
33) K. Kuniyoshi, K. Ozono, M. Ikeda, T. Suzuki, S. G. Kim and W. T. Kim: Sci. Tech. Adv. Maters. **7** (2006) 595.